Molecular Cell
Article

CDC-48/p97 Coordinates CDT-1 Degradation with GINS Chromatin Dissociation to Ensure Faithful DNA Replication

André Franz,[1] Michael Orth,[2] Paul A. Pirson,[1] Remi Sonneville,[3] J. Julian Blow,[3] Anton Gartner,[3] Olaf Stemmann,[2] and Thorsten Hoppe[1,*]
[1]Institute for Genetics and Cologne Excellence Cluster on Cellular Stress Responses in Aging-Associated Diseases (CECAD), University of Cologne, Zülpicher Strasse 47a, 50674 Cologne, Germany
[2]Department of Genetics, University of Bayreuth, Universitätsstrasse 30, 95440 Bayreuth, Germany
[3]Wellcome Trust Centre for Gene Regulation and Expression, College of Life Sciences, University of Dundee, Dow Street, Dundee DD1 5EH, UK
*Correspondence: thorsten.hoppe@uni-koeln.de
DOI 10.1016/j.molcel.2011.08.028

SUMMARY

Faithful transmission of genomic information requires tight spatiotemporal regulation of DNA replication factors. In the licensing step of DNA replication, CDT-1 is loaded onto chromatin to subsequently promote the recruitment of additional replication factors, including CDC-45 and GINS. During the elongation step, the CDC-45/GINS complex moves with the replication fork; however, it is largely unknown how its chromatin association is regulated. Here, we show that the chaperone-like ATPase CDC-48/p97 coordinates degradation of CDT-1 with release of the CDC-45/GINS complex. *C. elegans* embryos lacking CDC-48 or its cofactors UFD-1/NPL-4 accumulate CDT-1 on mitotic chromatin, indicating a critical role of CDC-48 in CDT-1 turnover. Strikingly, CDC-48$^{UFD-1/NPL-4}$-deficient embryos show persistent chromatin association of CDC-45/GINS, which is a consequence of CDT-1 stabilization. Moreover, our data confirmed a similar regulation in *Xenopus* egg extracts, emphasizing a conserved coordination of licensing and elongation events during eukaryotic DNA replication by CDC-48/p97.

INTRODUCTION

Accurate duplication of DNA is a central and challenging task in dividing cells that requires the hierarchical order of timely separated events (Bell and Dutta, 2002; Masai et al., 2010). In embryonic cell cycles, DNA replication starts during early mitosis with the loading of the prereplication complex (pre-RC) onto origins of replication (Budirahardja and Gönczy, 2009). The licensing factors CDT-1 and CDC-6 are central to this process because they bind to origins and subsequently recruit the replication helicase, the MCM complex, to complete pre-RC formation. For initiation of replication in late mitosis, pre-RCs are activated by phosphorylation for recruitment of essential replication factors, including CDC-45 and the Go-Ichi-Ni-San complex (GINS, representative for the subunits SLD-5, PSF-1, PSF-2, and PSF-3) (Ilves et al., 2010; Masuda et al., 2003; Mimura et al., 2000; Sheu and Stillman, 2006; Yabuuchi et al., 2006). As part of the active replisome, CDC-45 and GINS move with the replication fork during the elongation step of DNA synthesis (Aparicio et al., 2009; Gambus et al., 2006; Moyer et al., 2006; Pacek et al., 2006). To prevent reassembly of pre-RCs and thus reinitiation of DNA replication within the same cell cycle, CDT-1 is targeted for degradation at the start of the elongation phase by the CUL-4^{CDT-2} ubiquitin ligase in *C. elegans* (Havens and Walter, 2009; Zhong et al., 2003). This timely separation between DNA licensing and the elongation step of replication has been shown to be crucial for the maintenance of genome integrity (Takeda and Dutta, 2005). Remarkably, although the assembly steps have been studied in great detail, mechanisms that determine spatiotemporal dynamics of the replisome are largely unknown, especially once DNA replication has been completed.

Interestingly, our recent findings identified an essential role for the chaperone-like ATPase CDC-48 in DNA replication that is linked to cell-cycle progression (Deichsel et al., 2009; Mouysset et al., 2008). *C. elegans* CDC-48 and its orthologs in other species (termed Cdc48p in yeast and p97 in vertebrates) mediate mobilization and targeting of ubiquitylated proteins to the 26S proteasome (Rape et al., 2001). The substrate specificity is determined by different substrate-recruiting cofactors (Schuberth and Buchberger, 2008). For example, CDC-48/p97 cooperates with the UFD-1/NPL-4 heterodimer in endoplasmic reticulum (ER)-associated protein degradation (ERAD) and cell-cycle progression (Mouysset et al., 2006, 2008; Rabinovich et al., 2002). Depletion of the CDC-48$^{UFD-1/NPL-4}$ complex in worms causes severe defects in S phase progression of dividing cells, which depends on the DNA damage checkpoint. Moreover, reminiscent of the loss of the licensing factors CDT-1 and CDC-6, embryos lacking CDC-48, UFD-1, or NPL-4 are strongly reduced in DNA content. So far, interaction of CDC-48/p97 with DNA replication or repair proteins has been identified; however, the underlying mechanistic details remained unclear.

Here, we show a central regulatory role of CDC-48/p97 in the coordination of licensing and elongation events during eukaryotic DNA replication. *C. elegans* embryos lacking CDC-48 or its

cofactors UFD-1/NPL-4 accumulate CDT-1 on mitotic chromatin, implicating a yet unknown function of CDC-48 in CDT-1 degradation. Moreover, CDC-48$^{UFD-1/NPL-4}$-deficient embryos show persistent chromatin association of CDC-45/GINS after S phase is completed. Mechanistically, dissociation of CDC-45/GINS is a consequence of ubiquitin-dependent CDT-1 turnover regulated by CDC-48. Since we show similar results in *Xenopus* egg extracts, our findings demonstrate that the spatiotemporal coordination of CDT-1 degradation and GINS release is evolutionarily conserved, which is important for eukaryotic DNA replication and cell-cycle progression.

RESULTS

Chromatin Dissociation of CDC-45 and GINS Subunits Requires CDC-48$^{UFD-1/NPL-4}$

In early *C. elegans* embryonic cell cycles, S and M phases rapidly alternate without apparent gap phases, which can be monitored by time-lapse microscopy (Budirahardja and Gönczy, 2009). To characterize the mechanistic role of CDC-48 in DNA replication, we systematically analyzed the subcellular localization and dynamics of several conserved replication factors fused to green fluorescent protein (GFP) in *C. elegans* embryos that were depleted for the functional CDC-48$^{UFD-1/NPL-4}$ complex. During these experiments, chromatin was visualized by coexpression of mCherry-tagged histone H2B (mCherry::H2B). In wild-type embryos, CDC-45 and the GINS subunit SLD-5 similarly accumulate in the nucleus in S phase, but never colocalize with H2B on mitotic chromosomes. In contrast, codepletion of CDC-48.1 and CDC-48.2 by RNA interference (RNAi) (hereafter referred to as CDC-48 depletion or *cdc-48*(*RNAi*)) or depletion of its cofactors UFD-1/NPL-4 specifically affects the localization of GFP::CDC-45 and GFP::SLD-5. Time-lapse microscopy identified that CDC-45 and SLD-5 remain associated with chromatin throughout cell-cycle progression in *cdc-48*, *ufd-1*, and *npl-4* RNAi embryos (Figures 1A and 1B and Movies S1 and S2). In contrast, downregulation of *ufd-1* does not change the cellular distribution of the pre-RC proteins ORC-2 and CDC-6 or the DNA helicase subunit MCM-2 (Figure S1A). As CDC-48 is involved in additional biological processes cooperating with cofactors other than UFD-1/NPL-4, complete downregulation of CDC-48 blocks embryonic cell division (Mouysset et al., 2008; Sasagawa et al., 2007; Yamanaka et al., 2004). To specifically address the replication-related phenotype, we depleted *ufd-1* and/or *npl-4* in further experiments.

We have previously shown that CDC-48$^{UFD-1/NPL-4}$-depleted embryos exhibit a pronounced delay in S phase progression caused by activation of the DNA replication checkpoint kinases ATL-1/ATR and CHK-1/Chk1 (Abraham, 2001; Brauchle et al., 2003; Mouysset et al., 2008). Therefore, we tested whether activation of the replication checkpoint is responsible for the altered localization of CDC-45/GINS associated with the depletion of a functional CDC-48$^{UFD-1/NPL-4}$ complex. However, checkpoint activation caused by depletion of the DNA polymerase α subunit DIV-1 does not generate a comparable effect (Encalada et al., 2000) (Figure 1B). Whereas downregulation of *atl-1* suppresses the cell division delay of *ufd-1*(*RNAi*) embryos (Mouysset et al., 2008), it does not reverse the GFP::SLD-5 mislocalization (Figure 1B). Together, these data suggest that misregulation of the CDC-45/GINS complex is caused by CDC-48$^{UFD-1/NPL-4}$ depletion and is not a secondary effect of checkpoint activation.

Cell-Cycle Progression Defects of Embryos Lacking UFD-1 or NPL-4 Depend on CDC-45/GINS

We have shown that the CDC-48$^{UFD-1/NPL-4}$ complex is required for S phase progression of dividing cells of *C. elegans* embryos (Mouysset et al., 2008). The P0 zygote undergoes asymmetric division and generates an anterior AB cell and a smaller posterior P1 cell. These cells have different developmental fates and division timing, with AB dividing approximately 2 min before P1 (Encalada et al., 2000; Pellettieri and Seydoux, 2002). Downregulation of *cdc-48*, *ufd-1*, and *npl-4* activates the DNA damage checkpoint and further increases the cell division delay of P1 in comparison to AB, leading to a prolonged three-cell stage (Mouysset et al., 2008) (Figure 2A). Considering the persistent chromatin association, we tested the importance of CDC-45/GINS for the delayed S phase progression of embryos lacking CDC-48$^{UFD-1/NPL-4}$. To perform this experiment, we established an RNAi protocol to deplete UFD-1 or NPL-4 in the first place and subsequently deplete CDC-45 or different GINS subunits (Figure 2A). Indeed, depletion of *psf-3* or codepletion of both *cdc-45* and *sld-5* together significantly suppressed the P1 cell division delay of *ufd-1* and *npl-4* RNAi embryos (Figures 2B and 2C). Given that RNAi depletion of CDC-45/GINS on its own affects DNA replication and delays S phase, the suppression does not restore the cell division defect completely to the wild-type level. In contrast, RNAi-mediated downregulation of the DNA polymerase subunits DIV-1 and PRI-1 or the DNA repair protein RAD-51 (Wicky et al., 2004) had no effect or even increased the defect in cell-cycle progression of embryos lacking UFD-1 (Brauchle et al., 2003) (Figure S2A). To test whether depletion of CDC-45/SLD-5 is able to reduce S phase progression defects in general that are not linked to CDC-48, we used the *div-1(or148)* temperature-sensitive mutant that shows activation of the replication checkpoint at the restrictive temperature (Encalada et al., 2000). Strikingly, *cdc-45/sld-5* codepletion significantly enhanced rather than reduced the P1 delay phenotype of *div-1(or148)* (Figure S2B). Therefore, defective CDC-45/GINS regulation seems to contribute specifically to activation of the DNA replication checkpoint in embryos lacking a functional CDC-48$^{UFD-1/NPL-4}$ complex.

Recent data on the regulation of the RNA polymerase II subunit Rpb1 support the idea that CDC-48/p97 is frequently required to support degradation of chromatin-bound proteins (Verma et al., 2011). By yeast two-hybrid analysis, we identified a direct interaction between UFD-1 and CDC-45, suggesting a similar role in regulating the chromatin association of CDC-45/GINS (Figure 2D). Thus, we tested whether CDC-48$^{UFD-1/NPL-4}$-dependent regulation of CDC-45 and GINS subunits also determines their stability. However, the protein levels of CDC-45 and SLD-5 are not changed in *ufd-1*(*RNAi*) embryos (Figure 2E).

CDC-48$^{UFD-1/NPL-4}$ Is Required for CDT-1 Turnover at Mitotic Chromatin

Similar to *cdc-45*, *sld-5*, and *psf-3* depletion, downregulation of the licensing factor CDT-1 reduced the P1 cell division delay of

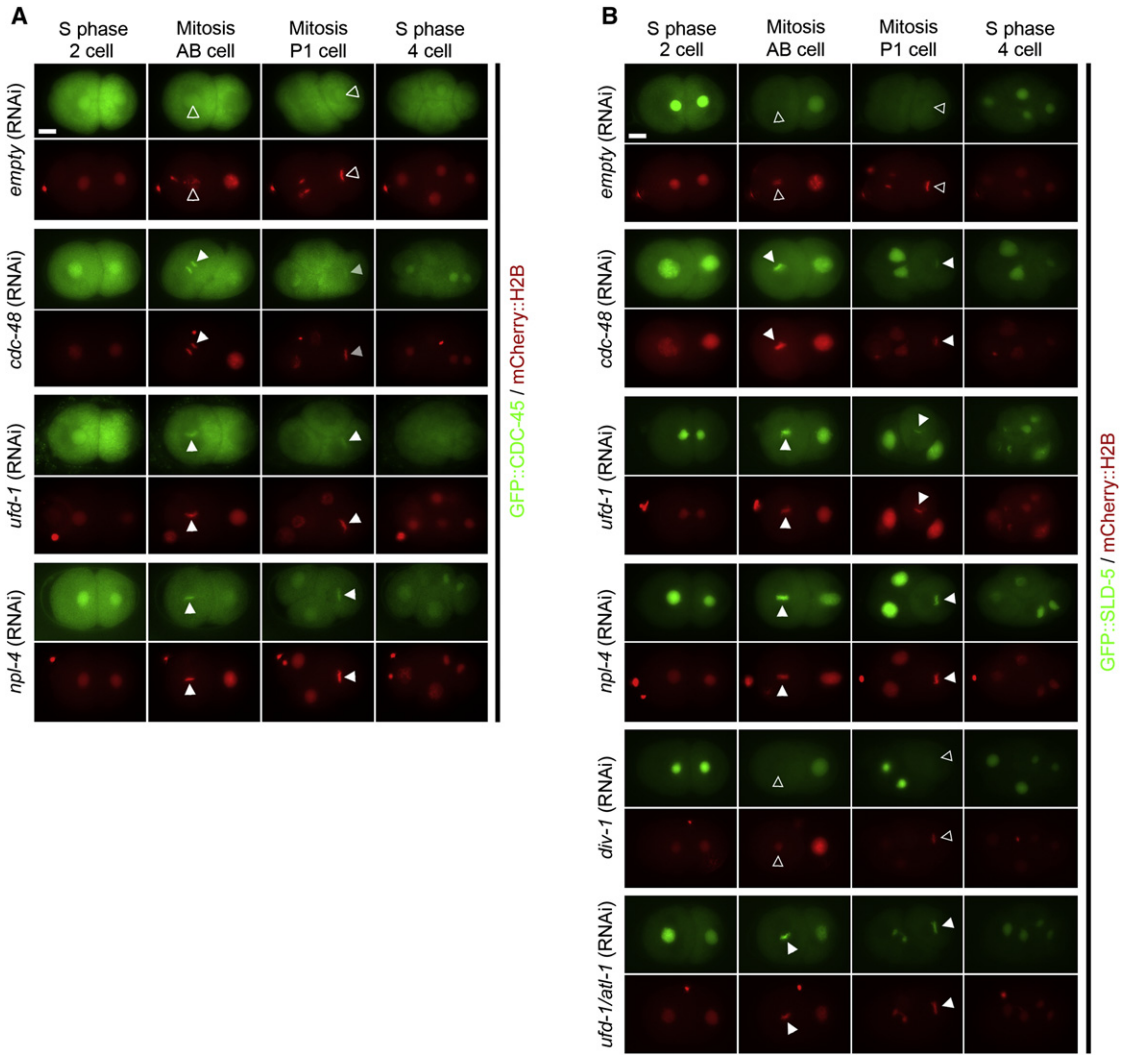

Figure 1. CDC-45 and Subunits of the GINS Complex Persist on Mitotic Chromatin in Embryos Depleted for the CDC-48$^{UFD-1/NPL-4}$ Complex
(A and B) Selected pictures of time-lapse recordings of embryos expressing GFP::CDC-45 or GFP::SLD-5 (green) and mCherry::H2B (red) that are depleted for *empty* control, *cdc-48* and/or *ufd-1*, *npl-4*, and *div-1* or codepleted for *ufd-1/atl-1* by RNAi. Each image series shows representative cell-cycle phases (mitosis or S phase) at distinct times of embryonic development (2–4 cell stage) of one single *C. elegans* embryo. Empty arrows indicate wild-type like mitotic localization, filled arrows indicate persistent association of the indicated proteins with mitotic chromatin. Anterior is to the left. Scale bars represent 5 μm.

ufd-1(RNAi) embryos (Figure 3A). Once per cell cycle, CDT-1 is involved in the initiation of the pre-RC at origins of replication. To maintain genome stability, CDT-1 is targeted for degradation by different E3 ligases subsequent to DNA licensing (Kim and Kipreos, 2007; Zhong et al., 2003). Therefore, we wondered whether the CDC-48$^{UFD-1/NPL-4}$ complex is also involved in the degradation of CDT-1. To clarify this hypothesis, *cdt-1* mRNA and CDT-1 protein levels were monitored in embryonic extracts depleted for *cdc-48*, *ufd-1*, *npl-4*, or *cdt-1* as control. Whereas *cdt-1* mRNA levels remained unchanged, quantification of the immunoblot and normalization with tubulin identified stabilization of CDT-1 upon downregulation of CDC-48, UFD-1, and NPL-4 (Figures 3B, 3C, S3A, and S3B). Given the high abundance of CDC-48 protein in cells (up to 1% of all cellular proteins [Peters et al., 1990]), RNAi treatment is not efficient enough to deplete CDC-48 completely in wild-type (Heubes and Stemmann, 2007). To solve this problem, we used the *cdc-48.1(tm544)* deletion mutant lacking one of two *C. elegans* genes encoding CDC-48 for complete downregulation (Figure 3C). In contrast to stabilization in embryos, CDT-1 did not accumulate significantly in whole worm lysates of a similar experiment, suggesting that CDT-1 degradation by the CDC-48$^{UFD-1/NPL-4}$ complex is especially important in actively dividing tissues (Mouysset et al., 2008).

In *C. elegans*, the SCF ligase subunit RBX-1 is required for CDT-1 degradation in somatic and germline cells (Jia et al., 2011). As we showed a role for the CDC-48$^{UFD-1/NPL-4}$ complex in CDT-1 turnover, we examined CDT-1 protein levels after downregulation of *ufd-1* and/or *rbx-1* to address epistatic effects. Surprisingly, codepletion of UFD-1 together with RBX-1 enhanced the stabilization of CDT-1 observed in single RNAi

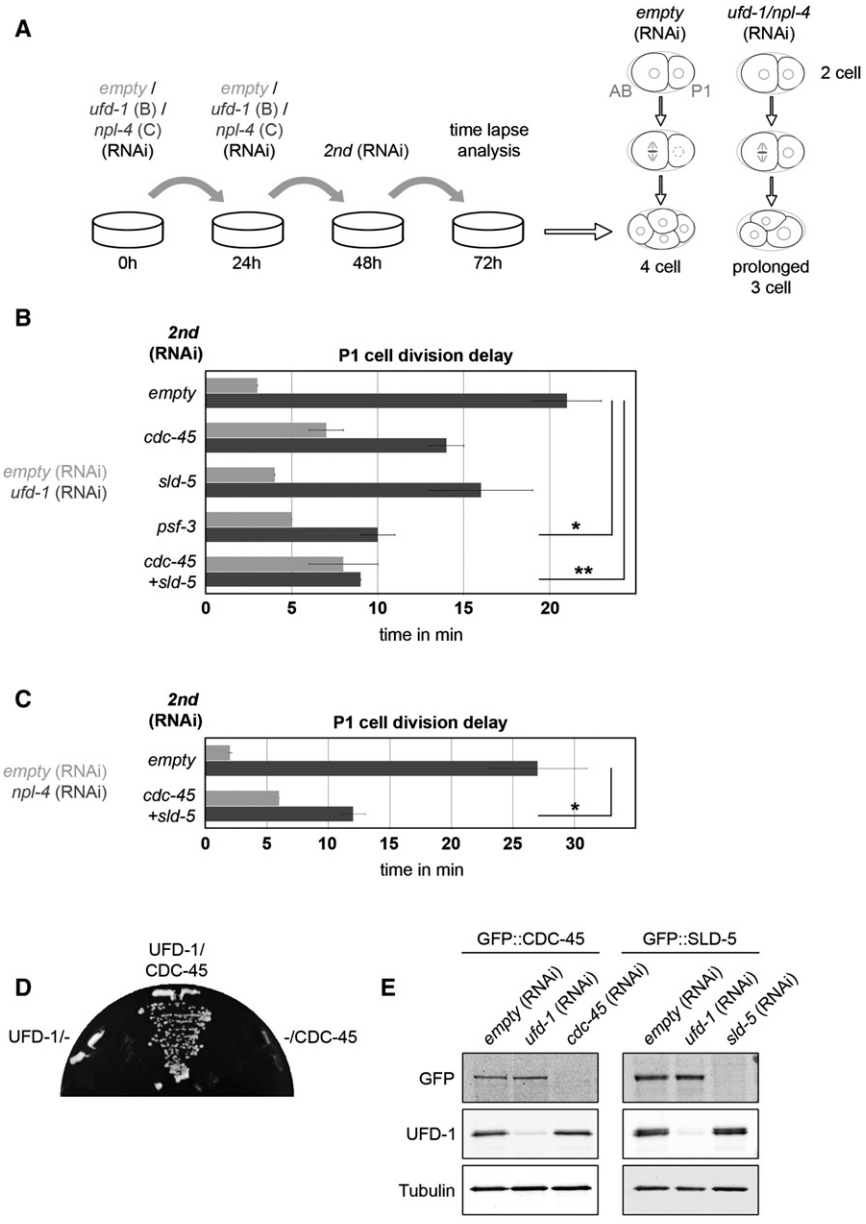

Figure 2. Suppression of the Cell-Cycle Progression Delay of Embryos Lacking UFD-1 or NPL-4 by *cdc-45*, *sld-5*, or *psf-3* RNAi Depletion

(A) Schematic illustration of the RNAi feeding procedure to achieve a sequential depletion of *empty* (light gray), *ufd-1*, or *npl-4* (dark gray) for the first 48 hr and *cdc-45*, *sld-5*, *psf-3*, or *cdc-45+sld-5* (2^{nd} RNAi) for the last 24 hr. Subsequent time-lapse analysis was performed to visualize the previously described delay of *ufd-1* and *npl-4* RNAi embryos in cell-cycle progression of the P1 cell (Mouysset et al., 2008).

(B and C) Quantification of the time between division of AB and P1 cell (P1 division delay) of embryos depleted first for *empty* (light gray) and *ufd-1* or *npl-4* (dark gray) and sequentially for *empty*, *cdc-45*, *sld-5*, and *psf-3* or codepleted for *cdc-45+sld-5* (2^{nd} RNAi).

(D) Two-hybrid assay for the interaction of *C. elegans* UFD-1 with CDC-45. Yeast cells expressing the indicated proteins were streaked out on medium plates lacking histidine to test for interaction-dependent activation of the *HIS3* gene.

(E) Western blot analysis of GFP fusions of CDC-45 and SLD-5 in *C. elegans* embryonic extracts depleted for *empty*, *ufd-1* and *cdc-45*, or *sld-5*.

Time is shown in hours (A) or minutes (B and C). Data are mean values. Error bars show standard error of the mean (SEM). Statistical significance between cell division timings are indicated by asterisks in (B) and (C). The single asterisk indicates $p \leq 0.05$ and the double asterisk indicates $p \leq 0.001$.

experiments, indicating that they might act in parallel degradation pathways (Figure 3D). Consistent with this observation, CDT-1 strongly accumulates on mitotic chromatin in *ufd-1* and *npl-4* RNAi embryos, but not in *rbx-1*(*RNAi*) or upon depletion of the Skp2 homolog SKPT-1, CUL-1/Cullin1, or the DNA replication/repair protein PCN-1/PCNA, which is required for CDT-1 degradation on chromatin (Havens and Walter, 2009). Stabilization of CDT-1 in nonsynchronized embryonic lysates lacking CDC-48, UFD-1, and NPL-4 appears mediocre but obvious given the low proportion of embryos undergoing mitosis, particularly when the progression through S phase is delayed (Figures 3B and 3C). In contrast to CDC-48, UFD-1, and NPL-4 depletion, CDT-1 is stabilized in S phase nuclei in *rbx-1* and *pcn-1* RNAi embryos (Figures 4A and 4B).

We addressed the importance of CDT-1 degradation for the chromatin association of CDC-45/GINS following GFP::SLD-5 localization during embryonic cell division. In contrast to CDC-$48^{UFD-1/NPL-4}$ downregulation, SLD-5 does not persist on mitotic chromatin upon depletion of RBX-1, PCN-1, SKPT-1, CUL-1, or the Cullin neddylation enzyme DCN-1 (Kurz et al., 2005) (Figures 1B, 4C, and S4B). This observation suggests that stabilization of CDT-1 in S phase does not affect CDC-45/GINS regulation. Consequently, CDC-$48^{UFD-1/NPL-4}$ defines CDT-1 degradation in mitosis, which is specifically linked to chromatin dissociation of the CDC-45/GINS complex.

Persistent Chromatin Binding of SLD-5 in *ufd-1*(*RNAi*) Embryos Depends on CDT-1

We tested the hypothesis that CDT-1 stabilization might directly affect GINS chromatin binding by quantification of chromatin-associated GFP::SLD-5 in embryos sequentially depleted for *ufd-1* or *ufd-1/cdt-1* (as described in Figure 2A). Importantly, depletion of *cdt-1* alone does not affect the localization of SLD-5, whereas depletion of *ufd-1* does. In contrast, sequential codepletion of *ufd-1* and *cdt-1* significantly reduced the amount of GFP::SLD-5 that remained bound to chromatin after S phase

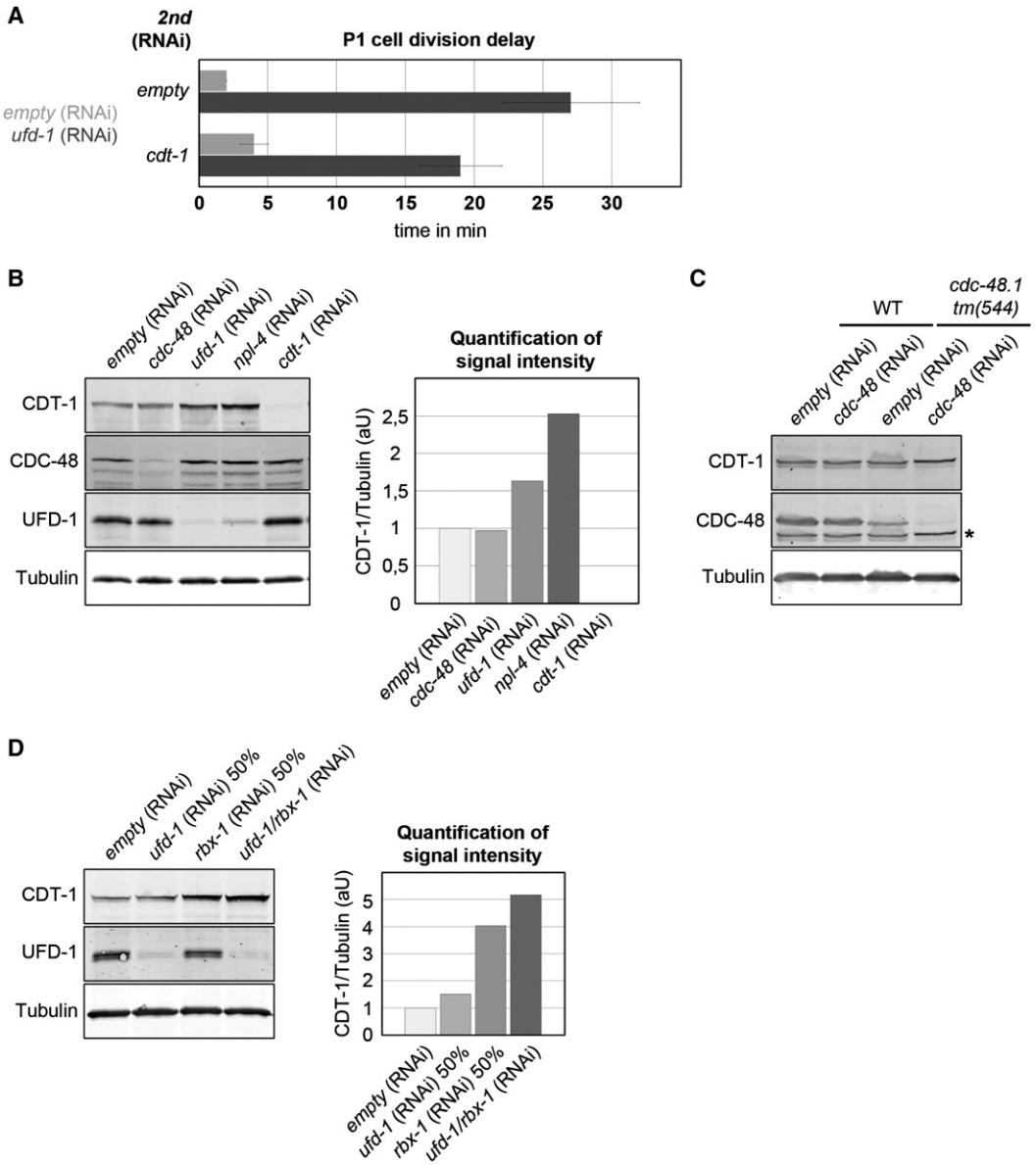

Figure 3. CDC-48$^{UFD-1/NPL-4}$-Depleted Embryos Show Elevated Levels of CDT-1 Protein

(A) Quantification of the cell division delay between AB and P1 cell (P1 division delay) of embryos depleted first for *empty* (light gray) or *ufd-1*(RNAi) (dark gray) and sequentially for *empty* or *cdt-1*(*RNAi*).

(B–D) Western blot analysis of CDT-1 protein levels in embryonic extracts that are depleted for the indicated gene products by RNAi. In (C), embryos were depleted for *empty* or *cdc-48(RNAi)* in wild-type or *cdc-48.1(tm544)* mutant background. In (D), *ufd-1* and *rbx-1*(*RNAi*) bacteria were equally mixed either with empty control bacteria or together. Quantification of the signal intensity was calculated relative to the tubulin level and normalized to the protein levels of the *empty*(*RNAi*) control. Time is shown in minutes (A). Data are mean values. Error bars show standard error of the mean (SEM).

(Figures 5A and 5B), indicating that GINS chromatin release and CDT-1 degradation are coordinated via CDC-48$^{UFD-1/NPL-4}$. We speculate that *cdt-1*(*RNAi*) for 24 hr affects the equilibrium between the free pool and chromatin-bound CDT-1 rather than reducing the CDT-1-dependent recruitment of CDC-45/GINS during the licensing process, whereas simultaneous downregulation of UFD-1 and CDT-1 together might completely block GINS recruitment (Figure S5A). Moreover, downregulation of the licensing factors ORC-2 and CDC-6 neither suppressed the cell-cycle progression phenotype of *ufd-1(RNAi)* nor reduced the amount of GFP::SLD-5 accumulating on mitotic chromatin in UFD-1-depleted embryos, which is in contrast to *cdt-1(RNAi)* (Figures 3A, 5A, 5B, S5B, and S5C).

CDC-48/p97-Dependent Regulation of GINS/Cdt1 Is Conserved in *Xenopus laevis*

To investigate whether CDC-48/p97 together with Ufd1/Npl4 is also required to coordinate GINS and Cdt1 regulation in

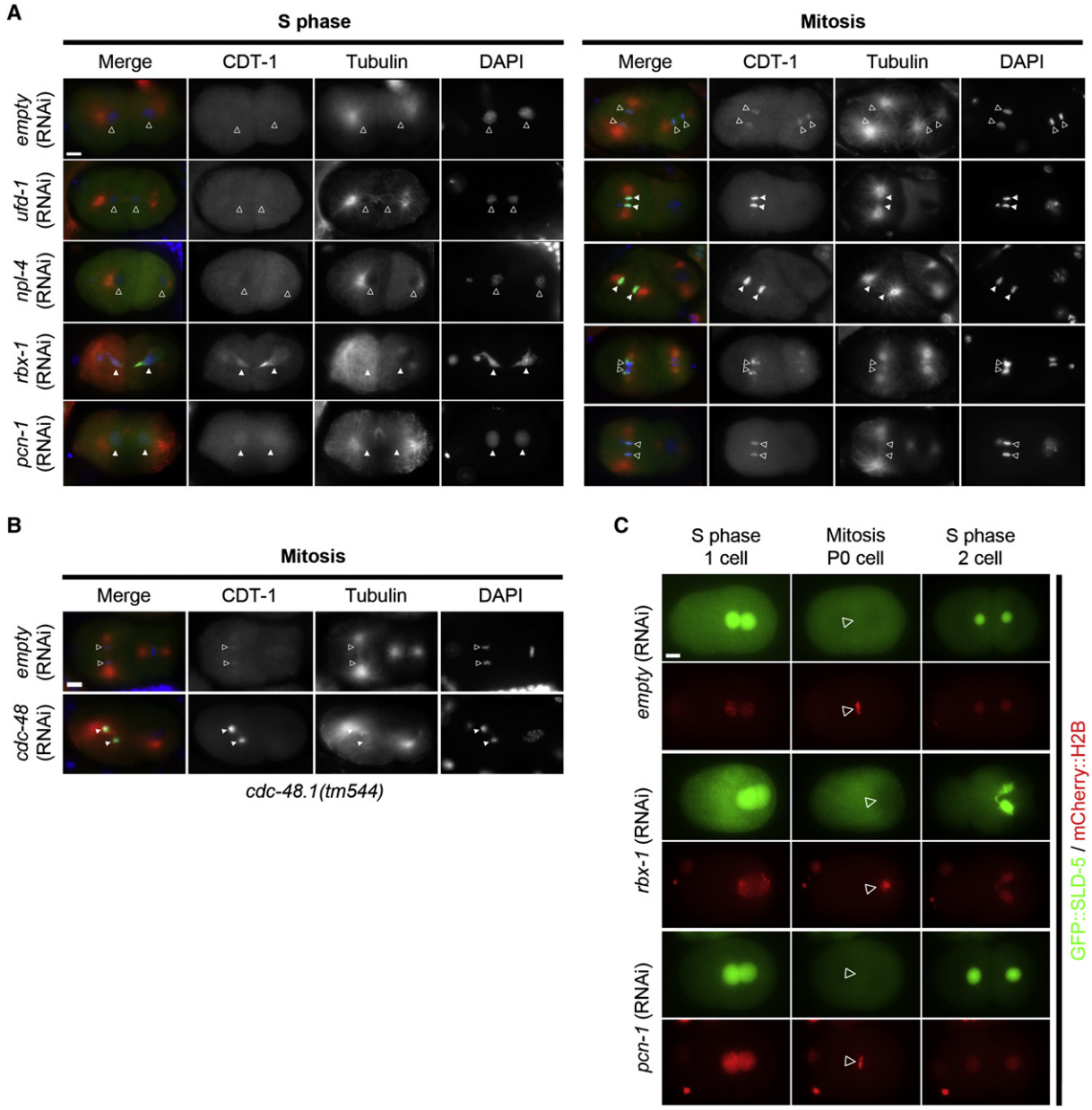

Figure 4. CDT-1 Accumulates on Mitotic Chromatin in *cdc-48*, *ufd-1*, and *npl-4* RNAi Embryos

(A and B) Immunostainings of early *C. elegans* embryos treated with *empty*, *cdc-48*, *ufd-1*, *npl-4*, *rbx-1*, or *pcn-1* (*RNAi*). CDT-1 (green), tubulin (red), and DAPI (blue) staining is shown as merge images and in separate channels. Distinct cell-cycle phases are indicated as mitosis or S phase. Empty arrowheads indicate wild-type CDT-1 levels, whereas filled arrowheads indicate enhanced signal intensity on mitotic chromatin. In (B), *cdc-48* (RNAi) was performed on *cdc-48.1(tm544)* mutant background.

(C) Selected pictures of time-lapse recordings of *C. elegans* embryos expressing GFP::SLD-5 (green) and mCherry::H2B (red) that are depleted for *empty* control, *rbx-1*, and *pcn-1*. Each image series shows representative cell-cycle phases of the first mitotic division of one single embryo. Empty arrowheads point to wild-type-like SLD-5 localization. Scale bar represents 5 μm.

vertebrates, we took advantage of the *Xenopus laevis* egg extract system to reisolate interphasic or mitotic chromatin and subsequently analyze associated proteins (Figure 6A). Remarkably, coimmunoprecipitation (coIP) experiments identified that Ufd1 interacts with Cdt1 in egg extracts, whereas Npl4 or the alternative p97 cofactor p47 does not. Since Npl4 also did not bind to p97 in this coIP, interaction with Cdt1 is likely to require p97 (Figure 6B). Furthermore, sequential pull-down of Ufd1 and His-tagged ubiquitin indicates interaction of ubiquitylated Cdt1 with Ufd1 (Figure 6C). Using affinity-purified antibodies (Heubes and Stemmann, 2007), we specifically depleted extracts from either Ufd1/Npl4 or p47 without affecting the

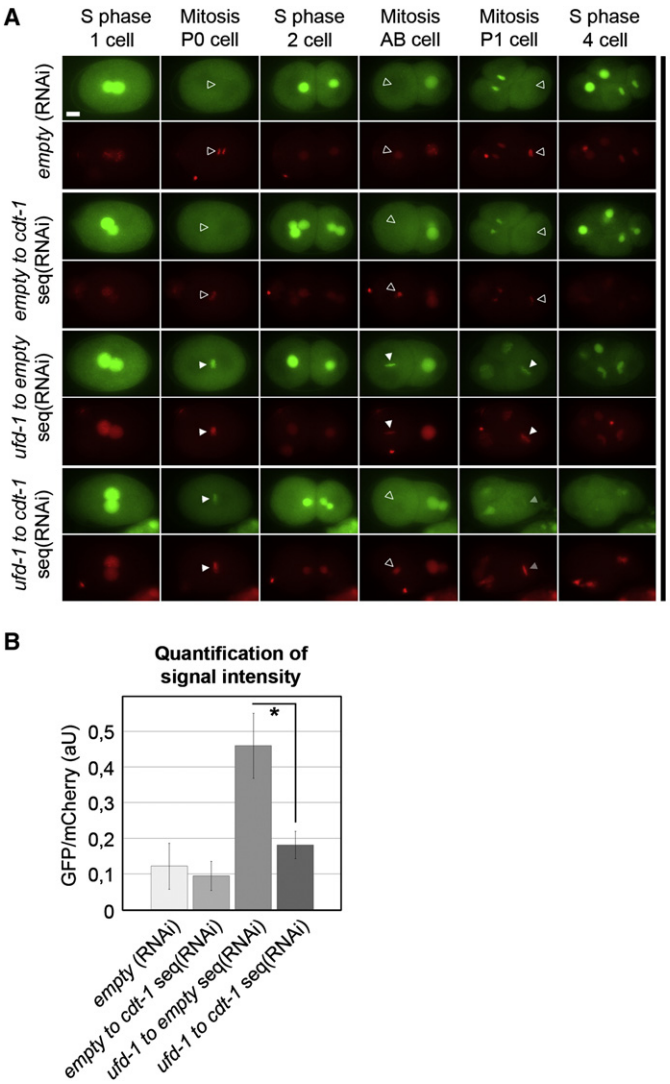

Figure 5. Depletion of CDT-1 Suppresses Persistent SLD-5 Chromatin Association in *ufd-1(RNAi)* Embryos

(A) Selected pictures of time-lapse recordings of embryos expressing GFP::SLD-5 (green) and mCherry::H2B (red) that are depleted first for *empty* or *ufd-1* followed by *empty* or *cdt-1* (*seq(RNAi)*). Representative pictures of indicated cell-cycle phases (mitosis or S phase) at distinct time points of embryonic development (1–4 cell stage) of one single *C. elegans* embryo are shown. Empty arrows indicate wild-type-like mitotic localization, filled arrows indicate persistent association with mitotic chromatin, and shaded arrowheads indicate partial mislocalization. Percentage values represent the number of mitotic divisions where SLD-5 chromatin association was monitored under indicated experimental conditions.

(B) Quantification of the GFP signal intensity on mitotic chromatin in embryos treated with *empty*, *cdt-1*, *ufd-1*, or *ufd-1/cdt-1 seq(RNAi)* shown in (A). GFP::SLD-5 signal intensity is shown relative to the intensity for mCherry::H2B in the same area. Anterior is to the left. Data are mean values. Error bars show standard error of the mean (SEM). Statistical significance of relative signal intensities are indicated by asterisks. The single asterisk indicates $p \leq 0.05$. Scale bar represents 5 μm.

overall p97 level (Figure 6D). The depleted extracts were released from CSF arrest by addition of calcium, and progression through interphase was then monitored via microscopy (Figure 6E). Eighty-five minutes after addition of calcium, interphase nuclei were observed for all extracts (Figure 6E, middle panel). The nuclei were reisolated from one half of the extracts, while the other half was driven back into mitosis for an additional 90 min. When extracts re-entered mitosis (Figure 6E, bottom panel), sperm chromatin was reisolated and examined for the presence of Cdt1/GINS both by immunofluorescence experiments and western blot analysis. Strikingly, we observed persistent binding of Sld5 and Cdt1 on mitotic chromatin isolated from Ufd1/Npl4-depleted extracts, which was not observed upon depletion of p47 (Figures 6F and 6G). As a component of the pre-RC, Cdt1 directly leaves chromatin after initiation of DNA replication (Maiorano et al., 2000). However, Cdt1 also accumulates on interphase chromatin specifically upon Ufd1/Npl4 depletion, which was isolated 85 min after calcium treatment when initiation has most likely occurred (Figure 6G, left part). In conclusion, these data suggest an evolutionarily conserved function of CDC-48/p97 in the degradation of Cdt1 linked to dissociation of GINS from chromatin, which seems to be important for accurate eukaryotic DNA replication.

DISCUSSION

Since CDC-48/p97 was identified as a crucial factor for cell-cycle progression in yeast, the precise role during cell division has remained unclear (Moir et al., 1982). Direct interaction with several factors involved in DNA metabolism has been reported in diverse organisms, which supports the recently described role of CDC-48 in DNA replication (Deichsel et al., 2009; Mouysset et al., 2008). Here, we discovered a conserved regulatory function of CDC-48/p97 in the coordination of licensing and elongation events during eukaryotic DNA replication both in *C. elegans* and *Xenopus laevis*. CDC-48$^{UFD-1/NPL-4}$-deficient embryos stabilize the licensing factor CDT-1 exclusively on mitotic chromatin (Figures 3B, 3C, 4A, and 4B). Furthermore, worm embryos lacking *cdc-48*, *ufd-1*, and *npl-4* show persistent CDC-45 and SLD-5 on chromatin, becoming visible on condensing chromosomes after S phase is completed (Figures 1A and 1B). Thus, our findings suggest that CDC-48/p97 orchestrates both CDT-1 degradation and chromatin dissociation of the CDC-45/GINS complex during eukaryotic DNA replication directly at the DNA. We show that downregulation of the licensing factors ORC-2 and CDC-6 neither suppressed the P1 division delay phenotype of *ufd-1(RNAi)* nor reduced the

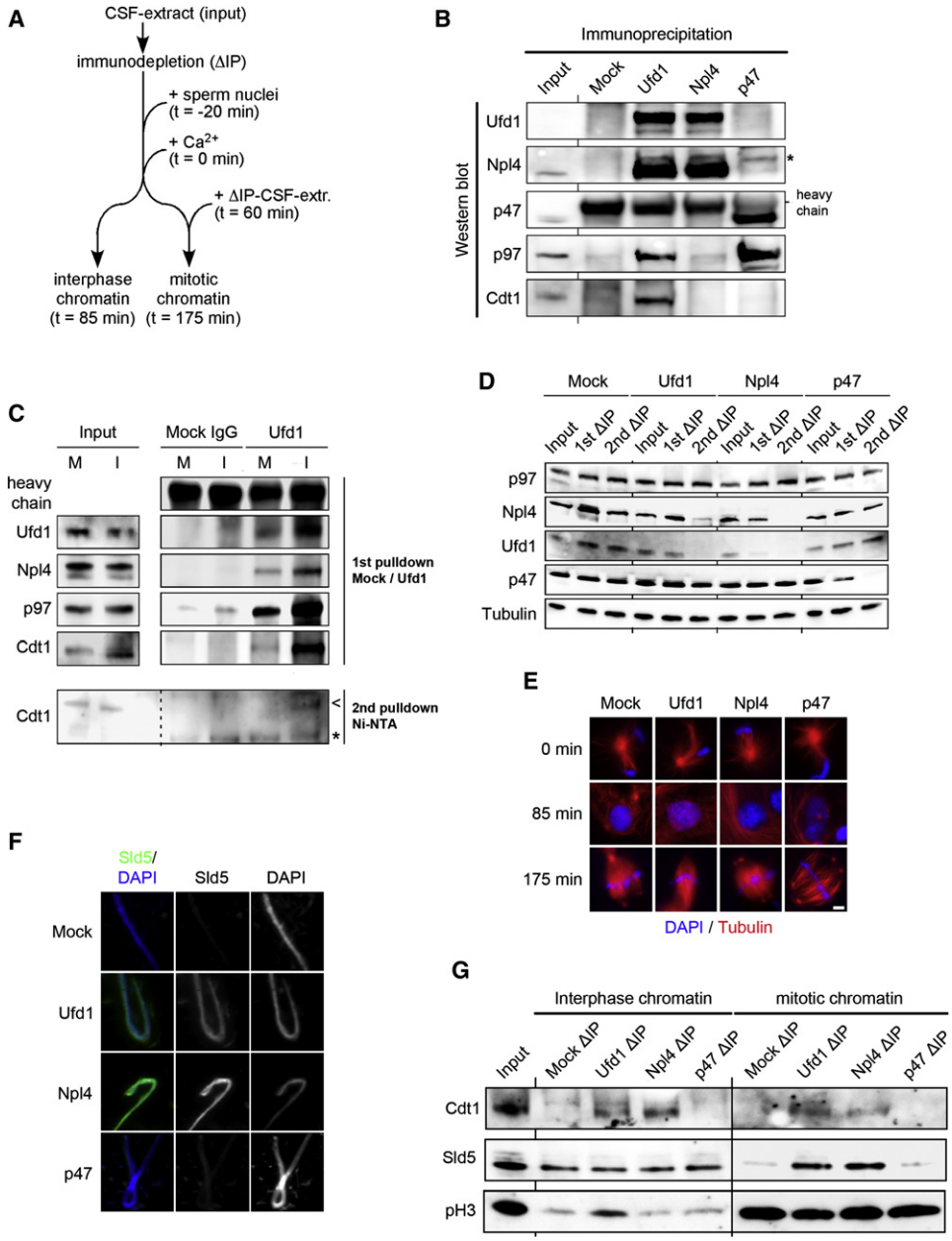

Figure 6. Regulation of Chromatin Association of GINS and Cdt1 Is Conserved in *Xenopus laevis* Egg Extracts

(A) Schematic illustration of the experimental procedure to reisolate sperm chromatin from S phase/interphase or mitotic *Xenopus* egg extracts.

(B) In vivo interaction between Ufd1 and Cdt1. *Xenopus* egg extracts were incubated with anti-Ufd1 antibodies coupled to protein A dynabeads for immunoprecipitation experiments.

(C) Two sequential pull-downs against unspecific IgG/Ufd1 and His-tagged Ubiquitin were performed from *Xenopus* egg extracts arrested in meiotic metaphase II (M) or interphase (I). Eluates were analyzed for the presence of indicated proteins by western blot. Cdt1 eluted from Ufd1 pull-downs can be precipitated by Ni-NTA (highlighted by <), indicating interaction of Ufd1 with ubiquitylated Cdt1. Asterisk indicates unspecific signal.

(D) Western blot analysis showing efficient immunodepletion of Ufd1, Npl4, and p47 after the first (1st IPΔ) and second (2nd IPΔ) round of incubation of egg extracts with the respective antibodies. Tubulin was used as loading control.

(E) Tubulin and DAPI staining of sperm chromatin incubated for 85 min or 175 min in mock control, Ufd1, Npl4, and p47 immunodepleted extracts show successive cycling through S phase/interphase and mitosis.

(F) Immunostaining of mitotic sperm chromatin that was incubated for 175 min in mock, Ufd1, Npl4, and p47 depleted egg extracts. Sld5 (green) and DAPI (blue) staining is shown as merge images and in separated channels.

(G) Western blot analysis of reisolated S phase/interphasic or mitotic sperm chromatin from mock, Ufd1, Npl4, and p47 depleted egg extracts. Cdt1 and Sld5 levels are shown. Phosphorylated Histone 3 was used as loading control.

amount of GFP::SLD-5, which accumulates on mitotic chromatin in UFD-1-depleted embryos, which is in contrast to *cdt-1(RNAi)* (Figures 3A, 3B, 5A, 5B, S5B, and S5C). Consequently, the reduction of chromatin-associated CDC-45/GINS in UFD-1-depleted embryos observed after *cdt-1(RNAi)* is not secondary to reduced recruitment of CDC-45/GINS during the licensing process. Therefore, the persistent association of CDC-45/GINS in embryos lacking UFD-1 and NPL-4 is specifically dependent on CDT-1 stabilization in late mitosis.

In contrast to CDC-48, RBX-1 and PCN-1 support CDT-1 degradation during S phase to prevent enhanced chromatin loading and rereplication (Figures 3D, 4A, and 4B) (Havens and Walter, 2009; Zhong et al., 2003). The fact that the GINS subunit SLD-5 does not persist on mitotic chromatin in the absence of *rbx-1* and *pcn-1* further supports the idea that stabilization of CDT-1 in S phase does not enhance CDC-45/GINS recruitment (Figures 1B and 4C). Unlike CDC-45/GINS, other replication factors known to be recruited by CDT-1 do not persist on chromatin in embryos lacking UFD-1 (Figure S1A). Therefore, we propose a highly specific role of CDC-48/p97 in the regulation of CDT-1 degradation in mitosis, which is linked to the dissociation of CDC-45/GINS. The misregulation of CDC-45/GINS seems to contribute to DNA replication defects in *cdc-48*, *ufd-1*, or *npl-4* RNAi embryos because depletion of CDC-45/SLD-5 and CDT-1 is able to suppress the P1 cell division delay of CDC-48$^{UFD\text{-}1/NPL\text{-}4}$-deficient embryos (Figures 2B, 2C, and 3A). However, given the significant delay in S phase progression still detectable in codepleted embryos, suppression of cell-cycle progression does not reflect restoration of DNA replication (Figure 2B).

Based on its function as a ubiquitin-selective chaperone, CDC-48/p97 is thought to provide segregase activity that separates ubiquitylated proteins from tightly bound partners (Ye, 2006). The best-studied segregase-like function is described for the ERAD pathway where CDC-48$^{UFD\text{-}1/NPL\text{-}4}$ mediates retranslocation of damaged proteins from the ER lumen to the cytosol for proteasomal degradation (Jarosch et al., 2002; Ye et al., 2001). Considering recent findings, it is intriguing to speculate that CDC-48/p97 especially extracts proteins from chromatin. For example, yeast Cdc48 is required for the turnover of the RNA polymerase II subunit Rpb1 upon DNA damage induction (Verma et al., 2011). In light of this observation, CDC-48/p97 probably facilitates extraction of ubiquitylated CDT-1 from mitotic chromatin, resulting in degradation of CDT-1 and dissociation of bound CDC-45/GINS subunits. Consequently, CDT-1/Cdt1 accumulates on mitotic chromatin of *C. elegans* embryos and *Xenopus* egg extract depleted for CDC-48, UFD-1/Ufd1, or NPL-4/Npl4 (Figures 3C, 4A, 6B, and 6G). In line with our data, Ballabeni et al. observed that in the absence of geminin, Cdt1 is ubiquitylated and degraded in mitosis, supporting the existence of a CDT-1/Cdt1 degradation pathway different from the known turnover pathway during S phase (Ballabeni et al., 2004). Stabilization of CDT-1 in mitosis might keep CDC-45/GINS tightly associated with chromatin, which may interfere with dynamic progression of the replication fork in S phase. Defects in GINS dissociation and DNA replication of *ufd-1*(*RNAi*) embryos are independent of ATL-1/CHK-1 and therefore not secondary to checkpoint activation (Figure 1B) (Mouysset et al., 2008). We propose that defects in CDC-45/GINS dissociation already take place in late mitosis/beginning of S phase but are first detectable with condensing chromosomes at the end of S phase (Figure 7). The CDC-48 complex seems to coordinate both events, since UFD-1/Ufd1 binds CDC-45 and Cdt1 (Figures 2D and 6B).

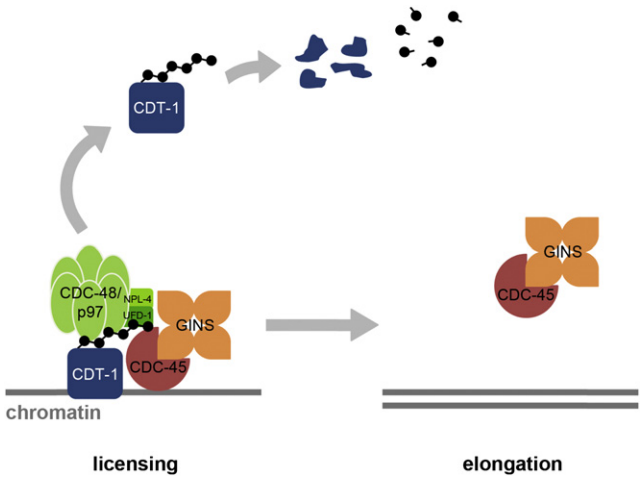

Figure 7. Hypothetical Model for the Coordination of CDT-1 Turnover and GINS Chromatin Extraction

CDC-48/p97, together with the cofactors UFD-1/NPL-4, coordinates the turnover of ubiquitylated CDT-1 during the licensing phase with chromatin dissociation of CDC-45/GINS. Failure in CDT-1 turnover keeps CDC-45/GINS tightly associated with chromatin, becoming visible with condensing chromosomes at the end of S phase. CDC-45/GINS misregulation may interfere with dynamic progression of the replication fork in S phase. The CDC-48/p97 complex seems to coordinate both events, since UFD-1/Ufd1 binds both CDC-45 and Cdt1.

Taken together, our findings show that the spatial and temporal regulation between dynamic protein complexes at the replication fork is governed by CDC-48/p97. In conclusion, CDC-48/p97 coordinates CDT-1 turnover and dissociation of the CDT-1-bound CDC-45/GINS complex, which is important for adjusting DNA replication and cell-cycle progression.

EXPERIMENTAL PROCEDURES

Strains

Worms were grown according to the standard protocols at 20°C, unless otherwise stated (Brenner, 1974). The *C. elegans* Bristol strain N2 was used as wild-type strain. Mutations and transgenes used in this study are listed as follows: *div-1(or148)III, cdc-48.1(tm544)II, unc-119(ed3)III; gtIs[unc-119(+), Ppie-1::GFP::mcm-2::pie-1-3′UTR], unc-119(ed3)III; gtIs[unc-119(+), Ppie-1::GFP::orc-2::pie-1-3′UTR], du[unc-119(+), Ppie-1::mCherry::H2B::pie-1-3′UTR], unc-119(ed3)III; gtIs[unc-119(+), Ppie-1::GFP::cdc-6::pie-1-3′UTR], du[unc-119(+), Ppie-1::mCherry::H2B::pie-1-3′UTR], unc-119(ed3)III; gtIs [unc-119(+), Ppie-1::GFP::cdc-45::pie-1-3′UTR], unc-119(ed3)III; gtIs[unc-119(+), Ppie-1::mCherry::H2B::pie-1-3′UTR], unc-119(ed3)III; gtIs[unc-119(+), Ppie-1::GFP::sld-5::pie-1-3′UTR], du[unc-119(+), Ppie-1::mCherry::H2B::pie-1-3′UTR], unc-119(ed3)III; [unc-119(+), Ppie-1::GFP::psf-3]*. The generation of *orc-2*, *cdc-6*, *mcm-2*, *cdc-45*, and *sld-5* transgenes fused to *gfp* and controlled by the *pie-1* promoter, as well as the detailed dynamic behavior of the respective fusion proteins and their biological validation, will be described elsewhere (R.S., J.J.B., and A.G., unpublished data).

RNAi

RNAi-mediated depletion was achieved using the feeding method (Kamath et al., 2001). RNAi was fed to L3/L4 larvae at 15°C for 72 hr. To induce stronger

expression of the fluorescent reporter constructs, worms were shifted to 20°C or 25°C overnight the day before time-lapse analysis. For sequential RNAi (*seq*(RNAi)) depletion, worms were fed with the dsRNA-containing bacteria against the first target gene for 48 hr and then switched to bacteria containing dsRNA against the second target. For the simultaneous depletion of two genes, the respective bacteria were mixed 1:1 in cell density. For the preparation of embryonic lysates, worms were kept at 20°C during the entire experimental procedure. In RNAi control experiments, bacteria contained only the empty vector pPD129.36.

Yeast Two-Hybrid Analysis

The full-length protein UFD-1 was fused to the GAL4 DNA binding domain using the vector pGBKT7 and coexpressed with CDC-45 fused to the GAL4 DNA activation domain using the vector pGADT7 in the yeast host strain AH109 (Clontech, Palo Alto, CA). Protein interaction studies were carried out according to the manufacturer's instructions.

Preparation of Embryonic Lysates

To produce embryonic lysates, L1 larvae were kept on control RNAi plates at 20°C until they reached the L3/L4 larval stage and then spread onto respective target RNAi plates. Embryos of gravid worms were harvested and resuspended in 2× Laemmli buffer. Embryos were sonicated twice for 15 s (Bandelin, Microtip MS 1.5), incubated at 95°C for 5 min, and centrifugated at 14,000 *g* for 5 min before SDS-PAGE analysis.

Microscopy and Image Acquisition

For time-lapse microscopy, embryos were mounted on agar pads essentially as described before (Mouysset et al., 2008). An AxioImager M1 microscope equipped with a AxioCam MRm camera (Carl Zeiss) was used for image acquisition. Time-lapse recordings in 90 s intervals were acquired using 2 × 2 mono binning to avoid photobleaching and toxicity. To allow direct comparison of signal intensities, images were recorded under identical conditions. Analysis of time-lapse recordings was done in the AxioVision 4.7 software. Timing of cell division was estimated as described previously (Mouysset et al., 2008). Processing of selected pictures was done in Adobe Photoshop CS4. Images of immunostainings were also acquired with AxioImager M1 and AxioCam MRm but using full resolution of the camera.

Immunotechniques

Immunostaining of early embryos was done essentially according to the "freeze-crack" protocol (Kemphues et al., 1986). Gravid worms were dissected onto polylysine-coated slides (Thermo Scientific) and frozen in liquid nitrogen, followed by incubation in −20°C methanol for 20 min and −20°C acetone for 5 min. After rehydration in PBS and blocking in 5% BSA, embryos were incubated with the primary antibody overnight at 4°C (anti-CDT-1 1:300, anti-α-tubulin 1:200 [Sigma, clone DM1A]). Incubation with the secondary antibodies (Alexa 488 or Alexa 594 conjugated, Invitrogen) was done at room temperature for 1 hr (1:400). Embryos were then mounted in DAPI Fluoromount G medium (SouthernBiotech). Quantification of signal intensities was done using ImageJ (National Institutes of Health). Background signal in the surrounding area was subtracted from values in the area of interest. For western blotting, proteins were separated by SDS-PAGE and transferred to nitrocellulose membranes (Whatman, Protran). Membranes were blocked in 3% milk solution and incubated with the primary antibodies overnight at 4°C in RotiBlock (Roth) (anti-CDT-1 1:300, anti-GFP 1:5,000 [Clontech], anti-tubulin 1:5,000 [Sigma, clone DM1A], anti-UFD-1 1:50,000, anti-CDC-48 1:50,000). Incubation with fluorescently labeled secondary antibodies (1:10,000) was done at room temperature, before detection of signals using the Li-Cor Odyssey scanner. Quantification of signal intensities was done using the Odyssey V3.0 software (Li-Cor). Background signal in the surrounding area was subtracted from values in the area of interest.

Xenopus laevis Egg Extract Preparation and Reisolation of Sperm Chromatin

CSF extracts were prepared as described previously (Murray, 1991). For immunodepletion, antibodies were coupled to Protein A Dynabeads (Invitrogen) overnight at 4°C. Extracts were depleted at 12°C in two rounds, each 30 min, as previously described (Heubes and Stemmann, 2007). After depletion, extracts were supplemented with rhodamine-labeled tubulin and sperm to a final concentration of 6000 nuclei/μl. Extracts were released from metaphase II arrest at 20°C by addition of Ca^{2+}, and cell-cycle stages were followed by fluorescence microscopy of fixed, Hoechst 33342-stained aliquots. Interphase extracts were split into halves. Sperm chromatin of one half was reisolated (see below) while the other half was driven back into mitosis by addition of an equal volume of depleted CSF extract. Reisolation of sperm chromatin was carried out as described previously (Stemmann et al., 2001).

Interaction Analysis of Ubiquitylated Cdt1 with Ufd1

CSF extract was prepared as described (Murray et al., 1991) and supplemented with sperm nuclei (4000 μl^{-1}) and His_6-tagged ubiquitin (2.5 μg/μl). To obtain interphase extract, half of the sample was released by addition of $CaCl_2$ to 0.6 mM and incubated for 20 min at 22°C. Then, CSF and interphase extracts were supplemented with cycloheximide (0.1 mg/ml), the proteasome inhibitor bortezomib (200 μM), and N-ethylmaleimide (10 mM). Antibodies (80 μg each) were coupled to magnetic protein A beads, and pull-downs from 1 ml of extract each were performed for 60 min at 12°C. Beads were washed three times with XB buffer supplemented with 300 mM NaCl and 0.1% Triton X-100. Precipitated proteins were eluted in 6M guanidiniumhydrochloride, 100 mM NaH_2PO_4, 10 mM Tris/HCl (pH 8.0), and 0.1% Triton X-100 and subjected to Ni-NTA pull-down for 3 hr at room temperature. Beads were washed five times in 8 M urea, 100 mM NaH_2PO_4, 10 mM Tris/HCl (pH 8.0), and 0.1% Triton X-100 and two times in PBS according to the protocol described by Siepe and Jentsch (Siepe and Jentsch, 2009). Proteins were eluted with SDS sample buffer at 95°C and analyzed by western blot.

Statistical Analysis

Statistical analysis was performed in Microsoft Excel. Statistical significance was calculated with two-tailed paired Student's t test. P values of $p \leq 0.05$ are indicated with a single asterisk, and double asterisks indicate $p \leq 0.001$. Comparison of cell division timings was done for experiments that were done on one single day, whereas Figure 2B shows summarized values for the controls of all experiments for better visualization.

SUPPLEMENTAL INFORMATION

Supplemental Information includes five figures, Supplemental Experimental Procedures, and two movies and can be found with this article online at doi:10.1016/j.molcel.2011.08.028.

ACKNOWLEDGMENTS

We thank A. Fire, E.T. Kipreos, M. Mechali, L. Pintard, H. Takisawa, the *Caenorhabditis* Genetics Center (funded by the NIH Center for Research Resources), the Dana-Farber Cancer Institute, and Geneservice Ltd. for antibodies, plasmids, cDNAs, and strains. We particularly thank J.W. Harper for exchange of unpublished results. We also thank A. Segref for critical reading of the manuscript. This work is supported by grants from the Deutsche Forschungsgemeinschaft (in particular by the CECAD, FOR885, SFB635, and DIP grant HO 2541/4-1 to T.H. and SPP1384 to O.S.), the Rubicon European Union Network of Excellence to T.H., Cancer Research UK program grant C303/A7399 to J.J.B., a Cancer Research UK CDA grant and a Wellcome Trust Senior Research Fellowship to A.G., and a postdoctoral EMBO fellowship to R.S. T.H. is an EMBO Young Investigator.

Received: April 6, 2011
Revised: June 22, 2011
Accepted: August 3, 2011
Published: October 6, 2011

REFERENCES

Abraham, R.T. (2001). Cell cycle checkpoint signaling through the ATM and ATR kinases. Genes Dev. *15*, 2177–2196.

Aparicio, T., Guillou, E., Coloma, J., Montoya, G., and Méndez, J. (2009). The human GINS complex associates with Cdc45 and MCM and is essential for DNA replication. Nucleic Acids Res. *37*, 2087–2095.

Ballabeni, A., Melixetian, M., Zamponi, R., Masiero, L., Marinoni, F., and Helin, K. (2004). Human geminin promotes pre-RC formation and DNA replication by stabilizing CDT1 in mitosis. EMBO J. *23*, 3122–3132.

Bell, S.P., and Dutta, A. (2002). DNA replication in eukaryotic cells. Annu. Rev. Biochem. *71*, 333–374.

Brauchle, M., Baumer, K., and Gönczy, P. (2003). Differential activation of the DNA replication checkpoint contributes to asynchrony of cell division in C. elegans embryos. Curr. Biol. *13*, 819–827.

Brenner, S. (1974). The genetics of Caenorhabditis elegans. Genetics *77*, 71–94.

Budirahardja, Y., and Gönczy, P. (2009). Coupling the cell cycle to development. Development *136*, 2861–2872.

Deichsel, A., Mouysset, J., and Hoppe, T. (2009). The ubiquitin-selective chaperone CDC-48/p97, a new player in DNA replication. Cell Cycle *8*, 185–190.

Encalada, S.E., Martin, P.R., Phillips, J.B., Lyczak, R., Hamill, D.R., Swan, K.A., and Bowerman, B. (2000). DNA replication defects delay cell division and disrupt cell polarity in early Caenorhabditis elegans embryos. Dev. Biol. *228*, 225–238.

Gambus, A., Jones, R.C., Sanchez-Diaz, A., Kanemaki, M., van Deursen, F., Edmondson, R.D., and Labib, K. (2006). GINS maintains association of Cdc45 with MCM in replisome progression complexes at eukaryotic DNA replication forks. Nat. Cell Biol. *8*, 358–366.

Havens, C.G., and Walter, J.C. (2009). Docking of a specialized PIP Box onto chromatin-bound PCNA creates a degron for the ubiquitin ligase CRL4Cdt2. Mol. Cell *35*, 93–104.

Heubes, S., and Stemmann, O. (2007). The AAA-ATPase p97-Ufd1-Npl4 is required for ERAD but not for spindle disassembly in Xenopus egg extracts. J. Cell Sci. *120*, 1325–1329.

Ilves, I., Petojevic, T., Pesavento, J.J., and Botchan, M.R. (2010). Activation of the MCM2-7 helicase by association with Cdc45 and GINS proteins. Mol. Cell *37*, 247–258.

Jarosch, E., Taxis, C., Volkwein, C., Bordallo, J., Finley, D., Wolf, D.H., and Sommer, T. (2002). Protein dislocation from the ER requires polyubiquitination and the AAA-ATPase Cdc48. Nat. Cell Biol. *4*, 134–139.

Jia, L., Bickel, J.S., Wu, J., Morgan, M.A., Li, H., Yang, J., Yu, X., Chan, R.C., and Sun, Y. (2011). RBX1 (RING box protein 1) E3 ubiquitin ligase is required for genomic integrity by modulating DNA replication licensing proteins. J. Biol. Chem. *286*, 3379–3386.

Kamath, R.S., Martinez-Campos, M., Zipperlen, P., Fraser, A.G., and Ahringer, J. (2001). Effectiveness of specific RNA-mediated interference through ingested double-stranded RNA in Caenorhabditis elegans. Genome Biol. *2*, H0002.

Kemphues, K.J., Wolf, N., Wood, W.B., and Hirsh, D. (1986). Two loci required for cytoplasmic organization in early embryos of Caenorhabditis elegans. Dev. Biol. *113*, 449–460.

Kim, Y., and Kipreos, E.T. (2007). Cdt1 degradation to prevent DNA re-replication: conserved and non-conserved pathways. Cell Div. *2*, 18.

Kurz, T., Ozlü, N., Rudolf, F., O'Rourke, S.M., Luke, B., Hofmann, K., Hyman, A.A., Bowerman, B., and Peter, M. (2005). The conserved protein DCN-1/Dcn1p is required for cullin neddylation in C. elegans and S. cerevisiae. Nature *435*, 1257–1261.

Maiorano, D., Moreau, J., and Méchali, M. (2000). XCDT1 is required for the assembly of pre-replicative complexes in Xenopus laevis. Nature *404*, 622–625.

Masai, H., Matsumoto, S., You, Z., Yoshizawa-Sugata, N., and Oda, M. (2010). Eukaryotic chromosome DNA replication: where, when, and how? Annu. Rev. Biochem. *79*, 89–130.

Masuda, T., Mimura, S., and Takisawa, H. (2003). CDK- and Cdc45-dependent priming of the MCM complex on chromatin during S-phase in Xenopus egg extracts: possible activation of MCM helicase by association with Cdc45. Genes Cells *8*, 145–161.

Mimura, S., Masuda, T., Matsui, T., and Takisawa, H. (2000). Central role for cdc45 in establishing an initiation complex of DNA replication in Xenopus egg extracts. Genes Cells *5*, 439–452.

Moir, D., Stewart, S.E., Osmond, B.C., and Botstein, D. (1982). Cold-sensitive cell-division-cycle mutants of yeast: isolation, properties, and pseudoreversion studies. Genetics *100*, 547–563.

Mouysset, J., Kähler, C., and Hoppe, T. (2006). A conserved role of Caenorhabditis elegans CDC-48 in ER-associated protein degradation. J. Struct. Biol. *156*, 41–49.

Mouysset, J., Deichsel, A., Moser, S., Hoege, C., Hyman, A.A., Gartner, A., and Hoppe, T. (2008). Cell cycle progression requires the CDC-48UFD-1/NPL-4 complex for efficient DNA replication. Proc. Natl. Acad. Sci. USA *105*, 12879–12884.

Moyer, S.E., Lewis, P.W., and Botchan, M.R. (2006). Isolation of the Cdc45/Mcm2-7/GINS (CMG) complex, a candidate for the eukaryotic DNA replication fork helicase. Proc. Natl. Acad. Sci. USA *103*, 10236–10241.

Murray, A.W. (1991). Cell cycle extracts. Methods Cell Biol. *36*, 581–605.

Murray, M.T., Krohne, G., and Franke, W.W. (1991). Different forms of soluble cytoplasmic mRNA binding proteins and particles in Xenopus laevis oocytes and embryos. J. Cell Biol. *112*, 1–11.

Pacek, M., Tutter, A.V., Kubota, Y., Takisawa, H., and Walter, J.C. (2006). Localization of MCM2-7, Cdc45, and GINS to the site of DNA unwinding during eukaryotic DNA replication. Mol. Cell *21*, 581–587.

Pellettieri, J., and Seydoux, G. (2002). Anterior-posterior polarity in C. elegans and Drosophila—PARallels and differences. Science *298*, 1946–1950.

Peters, J.M., Walsh, M.J., and Franke, W.W. (1990). An abundant and ubiquitous homo-oligomeric ring-shaped ATPase particle related to the putative vesicle fusion proteins Sec18p and NSF. EMBO J. *9*, 1757–1767.

Rabinovich, E., Kerem, A., Fröhlich, K.U., Diamant, N., and Bar-Nun, S. (2002). AAA-ATPase p97/Cdc48p, a cytosolic chaperone required for endoplasmic reticulum-associated protein degradation. Mol. Cell. Biol. *22*, 626–634.

Rape, M., Hoppe, T., Gorr, I., Kalocay, M., Richly, H., and Jentsch, S. (2001). Mobilization of processed, membrane-tethered SPT23 transcription factor by CDC48(UFD1/NPL4), a ubiquitin-selective chaperone. Cell *107*, 667–677.

Sasagawa, Y., Yamanaka, K., Nishikori, S., and Ogura, T. (2007). Caenorhabditis elegans p97/CDC-48 is crucial for progression of meiosis I. Biochem. Biophys. Res. Commun. *358*, 920–924.

Schuberth, C., and Buchberger, A. (2008). UBX domain proteins: major regulators of the AAA ATPase Cdc48/p97. Cell. Mol. Life Sci. *65*, 2360–2371.

Sheu, Y.J., and Stillman, B. (2006). Cdc7-Dbf4 phosphorylates MCM proteins via a docking site-mediated mechanism to promote S phase progression. Mol. Cell *24*, 101–113.

Siepe, D., and Jentsch, S. (2009). Prolyl isomerase Pin1 acts as a switch to control the degree of substrate ubiquitylation. Nat. Cell Biol. *11*, 967–972.

Stemmann, O., Zou, H., Gerber, S.A., Gygi, S.P., and Kirschner, M.W. (2001). Dual inhibition of sister chromatid separation at metaphase. Cell *107*, 715–726.

Takeda, D.Y., and Dutta, A. (2005). DNA replication and progression through S phase. Oncogene *24*, 2827–2843.

Verma, R., Oania, R., Fang, R., Smith, G.T., and Deshaies, R.J. (2011). Cdc48/p97 mediates UV-dependent turnover of RNA Pol II. Mol. Cell *41*, 82–92.

Wicky, C., Alpi, A., Passannante, M., Rose, A., Gartner, A., and Müller, F. (2004). Multiple genetic pathways involving the Caenorhabditis elegans Bloom's syndrome genes him-6, rad-51, and top-3 are needed to maintain genome stability in the germ line. Mol. Cell. Biol. *24*, 5016–5027.

Yabuuchi, H., Yamada, Y., Uchida, T., Sunathvanichkul, T., Nakagawa, T., and Masukata, H. (2006). Ordered assembly of Sld3, GINS and Cdc45 is distinctly regulated by DDK and CDK for activation of replication origins. EMBO J. *25*, 4663–4674.

Yamanaka, K., Okubo, Y., Suzaki, T., and Ogura, T. (2004). Analysis of the two p97/VCP/Cdc48p proteins of Caenorhabditis elegans and their suppression of polyglutamine-induced protein aggregation. J. Struct. Biol. *146*, 242–250.

Ye, Y. (2006). Diverse functions with a common regulator: ubiquitin takes command of an AAA ATPase. J. Struct. Biol. *156*, 29–40.

Ye, Y., Meyer, H.H., and Rapoport, T.A. (2001). The AAA ATPase Cdc48/p97 and its partners transport proteins from the ER into the cytosol. Nature *414*, 652–656.

Zhong, W., Feng, H., Santiago, F.E., and Kipreos, E.T. (2003). CUL-4 ubiquitin ligase maintains genome stability by restraining DNA-replication licensing. Nature *423*, 885–889.